

# Measurements of $\gamma\gamma \rightarrow$ Higgs and $\gamma\gamma \rightarrow W^+W^-$ in $e^+e^-$ collisions at the Future Circular Collider

DAVID D'ENTERRIA<sup>1</sup>

*CERN, EP Department 1211 Geneva, Switzerland*

PATRICIA REBELLO TELES<sup>2</sup>

*Centro Brasileiro de Pesquisas Físicas - CBPF, 22290-180 Rio de Janeiro, Brazil*

DANIEL E. MARTINS<sup>3</sup>

*Universidade Federal do Rio de Janeiro - UFRJ, 21941-901 Rio de Janeiro, Brazil*

The measurements of the two-photon production of the Higgs boson and of  $W^\pm$  boson pairs in  $e^+e^-$  collisions at the Future Circular Collider (FCC-ee) are investigated. The processes  $e^+e^- \xrightarrow{\gamma\gamma} e^+ H e^-, e^+ W^+W^- e^-$  are computed using the effective photon approximation for electron-positron beams, and studied in their  $H \rightarrow b\bar{b}$  and  $W^+W^- \rightarrow 4j$  decay final-states including parton showering and hadronization, jet reconstruction,  $e^\pm$  forward tagging, and realistic experimental cuts. After selection criteria, up to 75 Higgs bosons and 6600  $W^\pm$  pairs will be reconstructed on top of controllable continuum backgrounds at  $\sqrt{s} = 240$  and 350 GeV for the total expected integrated luminosities, by tagging the scattered  $e^\pm$  with near-beam detectors. A  $5\sigma$  observation of  $\gamma\gamma \rightarrow H$  is thereby warranted, as well as high-statistics studies of triple  $\gamma WW$  and quartic  $\gamma\gamma WW$  electroweak couplings, improving by at least factors of 2 and 10 the current limits on dimension-6 anomalous quartic gauge couplings.

PRESENTED AT

EDS Blois 2017 Conference , Prague,  
Czech Republic, June 26–30, 2017

---

<sup>1</sup>dde@cern.ch

<sup>2</sup>Speaker, patricia.rebello.teles@cern.ch

<sup>3</sup>dan.ernani@gmail.com

# 1 Introduction

After the Higgs boson discovery at the LHC [1, 2], subpercent precision studies of its couplings to all Standard Model (SM) particles, sensitive to scalar-coupled new physics in the multi-TeV range [3], require an electron-positron “Higgs factory” with high luminosities and low backgrounds running at center-of-mass (c.m.) energies of  $\sqrt{s} \approx 240\text{--}350$  GeV. Such conditions can be met in the  $e^+e^-$  mode of the Future Circular Collider (FCC-ee) [4], a post-LHC project under consideration at CERN, based on a 80-km circular ring aimed at eventually running proton-proton collisions up to c.m. energies of  $\sqrt{s} = 100$  TeV [5]. Among many important SM and beyond SM channels [4, 6], the large FCC-ee luminosities would make it feasible for the first time to observe with high rates the production of high-mass systems in photon-photon collisions thanks to the large effective fluxes of quasireal  $\gamma$ 's [7] radiated from the high-luminosity  $e^+e^-$  beams [8]. The two-photon production of the Higgs boson and of  $W^\pm$  pairs (Fig. 1, left) are both accessible at the FCC-ee and provide interesting tests of the SM electroweak sector. The former process provides an independent measurement of the  $H\text{-}\gamma$  coupling not based on Higgs decays but on its  $s$ -channel production mode, whereas the latter process probes trilinear  $\gamma W^+W^-$  and quartic  $\gamma\gamma W^+W^-$  electroweak couplings, and allows in particular to place competitive limits on anomalous quartic gauge couplings (aQGC) parametrized with dimension-6 and 8 effective operators of new physics at higher energy scales  $\Lambda$ , as done in pp collisions at the LHC [9]. Figure 1 (right) shows the  $\gamma\gamma$  effective

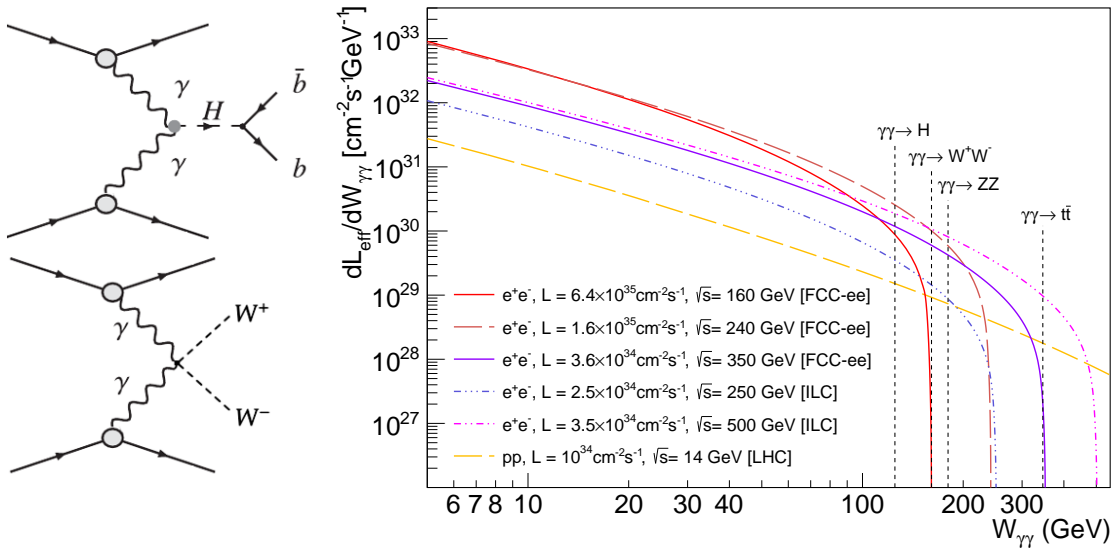


Figure 1: Left: Diagrams for the two-photon production of the Higgs boson (top) and  $W^\pm$  pairs (bottom). Right: Two-photon effective luminosities (EPA fluxes) as a function of  $\gamma\gamma$  c.m. energy over  $W_{\gamma\gamma} \approx 5\text{--}400$  GeV in  $e^+e^-$  collisions at FCC-ee and ILC, and in pp collisions at the LHC.

tive luminosities ( $\mathcal{L}_{\text{eff}}$ ) as a function of photon-photon c.m. energy  $W_{\gamma\gamma}$ , obtained from the convolution of the corresponding effective photon approximation (EPA) fluxes [7] with the

collider luminosities at various planned  $e^+e^-$  colliders (FCC-ee, ILC) and in pp collisions at the LHC. Except for electromagnetic (ultraperipheral) ion-ion collisions at the FCC [10], the FCC-ee features the largest effective two-photon luminosities for masses  $W_{\gamma\gamma} \lesssim 200$  GeV, with the advantage of the absence of pile-up collisions.

In this work, feasibility studies for the measurement of photon-fusion production of the Higgs boson in its  $b\bar{b}$  decay channel, and of  $W^\pm$  boson pairs decaying into four jets are presented. Observing both fully-hadronic exclusive final-states is unfeasible at the LHC due to the large pp pileup conditions and the lack of (420 m) proton taggers in the tunnel with a good acceptance in the  $\mathcal{O}(100$  GeV) mass region [11]. Compared to our previous studies [8], several improvements have been implemented. First, instead of using MADGRAPH 5 [12] the events are now generated with the latest versions of PYTHIA 8 [13] and SUPERCHIC v2 [14], keeping the exact kinematics information of the scattered  $e^\pm$ ; showering and hadronization of the final-state quarks are taken care by PYTHIA 6 or 8; and jets are reconstructed with FASTJET. Second, the  $e^\pm$  tagging conditions have been changed. Previously, the requirement to observe the scattered  $e^\pm$  within the instrumented central detector reduced significantly the visible cross sections. Our approach now, is to tag the outgoing  $e^\pm$  in near-beam detectors inside the FCC-ee tunnel, as done at the LHC for the proton-proton case [15]. Requiring double  $e^\pm$  tagging within  $1^\circ$  of the beam line, increases significantly the acceptance for both  $\gamma\gamma$  processes: 75%, 95% and 98.5% for Higgs production at  $\sqrt{s} = 160, 240,$  and  $350$  GeV respectively, although a realistic study of the FCC-ee beam optics is needed in order to determine the exact position of such  $e^\pm$ -taggers in the tunnel.

## 2 Theoretical setup

Event generation for the two-photon signal processes  $e^+e^- \xrightarrow{\gamma\gamma} e^+ H(b\bar{b})e^-$ ;  $e^+ W^+W^-(4j)e^-$ , (as well as the corresponding  $\gamma\gamma$  backgrounds) is carried out with SUPERCHIC 2.04 [14] and/or PYTHIA 8.226 [13] Monte Carlo (MC) codes, where the cross sections are obtained from the convolution of the corresponding EPA photon fluxes with the  $\gamma H$ ,  $\gamma WW$ ,  $\gamma\gamma WW$  vertices described by matrix elements (effective ones, in the  $\gamma H$  case) and exact kinematics. The virtuality of both photons is constrained to be in the quasireal range,  $Q^2 < 2$  GeV<sup>2</sup>. Both MC event generators yield consistent cross sections for the same processes. Non-photon-induced backgrounds from  $e^+e^-$  collisions sharing the same final-states as the signals of interest are generated with PYTHIA 6.4 [16] or PYTHIA 8.226. Initial and final state radiation (ISR, FSR), parton showering, hadronization, and decays are handled also by any of the two PYTHIA codes. The jets of hadrons resulting from the fragmentation of the produced partons are reconstructed using the  $e^+e^- k_t$  Durham algorithm [17] with the FASTJET 3.0 library [18].

### 3 $\gamma\gamma \rightarrow H \rightarrow b\bar{b}$ results

Figure 2 (left) shows the energy-dependence of the cross sections for the “standard” Higgsstrahlung and W,Z boson fusion (VBF) production mechanisms computed with HZHA [19], compared to  $\gamma\gamma$  production (bottom curve) in the range of FCC-ee energies. Two-photon Higgs production has the smallest cross sections, amounting to about 25, 90, and 200 ab at  $\sqrt{s} = 160, 240,$  and  $350$  GeV respectively, which would still lead to the production of 130–300 scalar bosons thanks to the large total integrated luminosities expected at each c.m. energy ( $\mathcal{L}_{\text{int}} \approx 10, 5, 1 \text{ ab}^{-1}$  respectively). Of course, the visible number of Higgs bosons is smaller

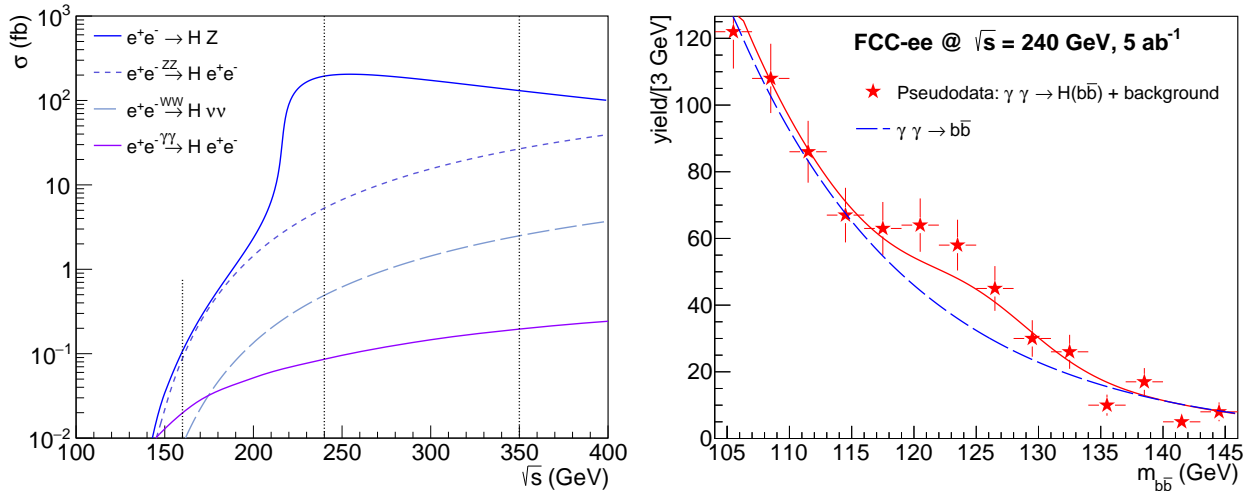


Figure 2: Left: Contributions to the Higgs boson cross section in  $e^+e^-$  collisions (unpolarized beams, ISR included) as a function of c.m. energy: HZ and VBF (via ZZ and WW exchanges) computed with HZHA [19], and photon-fusion computed with SUPERCHIC 2.04 [14]. The vertical lines indicate the FCC-ee energies of  $\sqrt{s} = 160, 240,$  and  $350$  GeV. Right: Expected dijet invariant mass distribution for two-photon Higgs signal and  $b\bar{b}$  continuum, in  $5 \text{ ab}^{-1}$  of  $e^+e^-$  collisions at  $\sqrt{s} = 240$  GeV, after  $e^\pm$  tagging and simple cuts in the b-jet pseudorapidities (see text).

after accounting for decay branching ratios, reconstruction performance, and analysis cuts to reduce backgrounds. The dominant Higgs decay mode is  $H \rightarrow b\bar{b}$ , with 58% branching fraction [20], and thereby the channel with the largest number of counts expected. Signal and background events for the  $\gamma\gamma \rightarrow H \rightarrow b\bar{b}$  measurement are simulated with PYTHIA 8.226, with FASTJET 3.0 being used to reconstruct two exclusive jets final-states. Reducible backgrounds, dominated by the process  $e^+e^- \rightarrow Z^*/\gamma^* \rightarrow b\bar{b}$  with a cross section of  $\sigma \approx 2 \text{ pb}$  over the mass range  $m_{b\bar{b}} = 100\text{--}150$  GeV, can be completely removed by requiring the double  $e^\pm$  tagging at polar angles  $\theta_{e^\pm} < 1^\circ$ . At 160, 240, and 350 GeV, double-tagging saves 75%, 95%, and 98.5% of the two-photon Higgs signal, while it also completely gets rid of the  $e^+e^- \xrightarrow{ZZ} e^+ H e^-$  process (second dominant curve in Fig. 2, left) which features outgoing  $e^\pm$  at much central rapidities. The irreducible background from the  $\gamma\gamma \rightarrow b\bar{b}$  continuum is 30–40

times larger than the signal over masses  $100 < W_{\gamma\gamma} < 150$  GeV, but can be suppressed (as well as that from misidentified  $c\bar{c}$  and  $q\bar{q}$  pairs) via various kinematical cuts. The data analysis follows the similar approach described in [21]. The following reconstruction performances have been assumed: jets reconstructed over  $|\eta| < 5$ , 7%  $b$ -jet energy resolution (resulting in a dijet mass resolution of  $\sim 6$  GeV at the Higgs peak), 75%  $b$ -jet tagging efficiency, and 5% (1.5%)  $b$ -jet mistagging probability for a  $c$  (light-flavour  $q = uds$ ) quark. For the double  $b$ -jet final-state of interest, these lead to a  $\sim 56\%$  efficiency for the pure generated signal (S), and a total reduction of the misidentified  $c\bar{c}$  and  $q\bar{q}$  continuum backgrounds (B) by factors of  $\sim 400$  and  $\sim 400\,000$ , respectively (Table 1).

Table 1: Summary of the visible cross sections for signal and backgrounds in the  $\gamma\gamma \rightarrow H(b\bar{b})$  analysis, obtained from PYTHIA 8 simulations in  $e^+e^-$  collisions at  $\sqrt{s} = 160, 240$  GeV and 350 GeV, after applying various selection criteria.

Process	$\sqrt{s}$ (GeV)	$[m_{jj} = 100\text{--}150 \text{ GeV}]$ ( $b$ -jet (mis)tag efficiency)	$\dots$ $\dots$ $e^\pm$ -tag $ \eta^j  < 1$	$\dots$ $\dots$ $\dots$ $\dots$ $[m_{jj} = 117\text{--}133 \text{ GeV}]$
$\gamma\gamma \rightarrow H \rightarrow b\bar{b}$	160	13.2 (7.4) ab	4.0 ab	3.3 ab
$\gamma\gamma \rightarrow b\bar{b}$		547. (308.) ab	41. ab	13.5 ab
$\gamma\gamma \rightarrow c\bar{c}$		13.2 fb (33. ab)	3.0 ab	0.92 ab
$\gamma\gamma \rightarrow q\bar{q}$		18.5 fb (4.2 ab)	0.34 ab	0.12 ab
$\gamma\gamma \rightarrow H \rightarrow b\bar{b}$	240	58.0 (32.6) ab	17.7 ab	14.9 ab
$\gamma\gamma \rightarrow b\bar{b}$		2.05 (1.15) fb	125. ab	52.2 ab
$\gamma\gamma \rightarrow c\bar{c}$		4.95 fb (124 ab)	9.2 ab	3.71 ab
$\gamma\gamma \rightarrow q\bar{q}$		69.5 fb (15.6 ab)	0.94 ab	0.37 ab
$\gamma\gamma \rightarrow H \rightarrow b\bar{b}$	350	130. (73.1) ab	30.3 ab	25.5 ab
$\gamma\gamma \rightarrow b\bar{b}$		4.38 (2.47) ab	204. ab	96.7 ab
$\gamma\gamma \rightarrow c\bar{c}$		106. fb (264. ab)	14.6 ab	6.92 ab
$\gamma\gamma \rightarrow q\bar{q}$		147. fb (33.1 ab)	1.5 ab	1.06 ab

Various simple kinematical cuts can be applied to enhance the S/B ratio. The Higgs boson is produced in the  $s$ -channel and its associated decay  $b$ -jets, emitted isotropically, have pseudorapidities peaking around  $\eta^j \approx 0$ , whereas the continuum – with quarks propagating in the  $t$ - or  $u$ - channels – are more peaked in the forward and backward directions. Simply requiring both jets to have pseudorapidities  $|\eta^j| < 1$  reduces the signal by 30–50%, while removing 80–90% of the backgrounds. The significance of the signal can be computed from the resulting number of counts within  $1.4\sigma$  around the Gaussian Higgs peak (*i.e.*  $117 < m_{b\bar{b}} < 133$  GeV) over the underlying exponential dijet continuum. At  $\sqrt{s} = 240$  GeV, for a total integrated luminosity of  $\mathcal{L}_{\text{int}} = 5 \text{ ab}^{-1}$  (3 years, 2 interaction points), we expect about

75 signal counts over 275 for the sum of backgrounds, reaching a statistical significance close to  $5\sigma$  (Fig. 2, right). Similar estimates for 160 GeV ( $10 \text{ ab}^{-1}$ ) and 350 GeV ( $1 \text{ ab}^{-1}$ ) yield  $3\sigma$  significances for the evidence of  $\gamma\gamma \rightarrow \text{H}$  production. Of course, those numbers are based on a simple set of kinematical cuts. A multivariate analysis exploiting many other kinematical properties of signal and backgrounds would easily improve such results.

#### 4 $\gamma\gamma \rightarrow \text{W}^+\text{W}^- \rightarrow 4\text{j}$ results

The SUPERCHIC v2.04 code is used for event generation of  $\text{W}^+\text{W}^-$  pairs in  $e^+e^-$  at  $\sqrt{s} = 240, 350 \text{ GeV}$  in the phase space region given by  $W_{\gamma\gamma} > 161 \text{ GeV}$ . The two bosons, decayed, showered, and hadronized with PYTHIA 8.226, are reconstructed as a four exclusive jets final-state. The dominant background from the process  $e^+e^- \rightarrow 4\text{j}$  with  $\sigma \approx 8.8 \text{ pb}$ , is fully suppressed with double  $e^\pm$  tagging ( $\theta_{e^\pm} < 1$ ), leaving as irreducible background only the  $\gamma\gamma \rightarrow 4\text{j}$  continuum process (simulated with PYTHIA 6.4) which can be easily removed applying a few simple kinematical cuts (Table 2). Requiring all jets to have  $p_T > 10 \text{ GeV}$ ,  $|\eta^j| < 2.5$ , and be separated by  $\Delta R^j > 0.4$  reduces by  $\sim 97\%$  the background for a  $\sim 25\%$  loss of the signal. Figure 3 compares the relevant differential distributions for signal and irreducible background in  $e^+e^-$  at  $\sqrt{s} = 240 \text{ GeV}$  before (top) and after (bottom) applying the selection criteria. Requiring, in addition, each pair of jets to have an invariant mass around the W value ( $m_{jj} = 76.5\text{--}84.5 \text{ GeV}$ ) further improves the signal over background (last column of Table 2). At  $\sqrt{s} = 240, 350 \text{ GeV}$  with total integrated luminosities of  $\mathcal{L}_{\text{int}} \approx 5$  and  $1 \text{ ab}^{-1}$ , we would therefore expect about 4400 and 6600 signal events, respectively, over much smaller backgrounds.

Table 2: Summary of the visible cross sections for signal and backgrounds in the  $\gamma\gamma \rightarrow \text{W}^+\text{W}^- \rightarrow 4\text{-jets}$  analysis, obtained with SUPERCHIC 2.04 (plus PYTHIA 8) and PYTHIA 6 simulations in  $e^+e^-$  at  $\sqrt{s} = 240 \text{ GeV}$  and  $350 \text{ GeV}$ , after applying various selection criteria.

Process	$\sqrt{s}$	cross section (incl. $e^\pm$ -tag)	...	...
			$p_T^j > 10\text{GeV}$	...
			$ \eta^j  < 2.5$	...
			$\Delta R^{jj} > 0.4$	...
				$[m_{jj} = 76.5\text{--}84.5 \text{ GeV}]$
$\gamma\gamma \rightarrow \text{W}^+\text{W}^- \rightarrow 4\text{jets}$	240 GeV	1.64 (1.43) fb	1.10 fb	0.87 fb
$\gamma\gamma \rightarrow 4\text{jets}$		10.49 (9.12) fb	0.27 fb	0.10 fb
$\gamma\gamma \rightarrow \text{W}^+\text{W}^- \rightarrow 4\text{jets}$	350 GeV	10.5 (10.2) fb	7.7 fb	6.61 fb
$\gamma\gamma \rightarrow 4\text{jets}$		46.9 (45.4) fb	1.3 fb	0.52 fb

A preliminary study based on an implementation of dimension-6  $\gamma\gamma\text{WW}$  operators in MADGRAPH 5 (v2.5.4) [12], indicates that using the  $p_T$  of the leading jet and the invariant

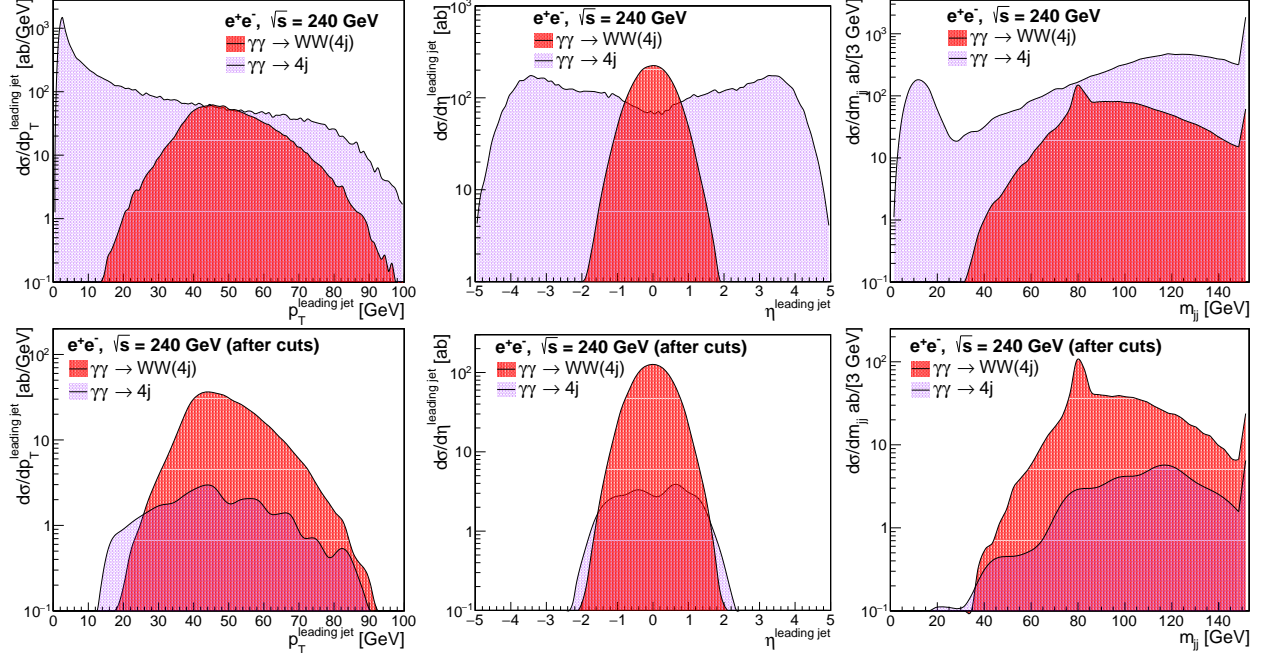


Figure 3: Relevant kinematical distributions for  $\gamma\gamma \rightarrow WW$  signal and  $\gamma\gamma \rightarrow 4j$  background in  $e^+e^-$  collisions at  $\sqrt{s} = 240$  GeV:  $p_T$  (left) and  $\eta$  (middle) of the leading jet, and invariant mass  $m_{jj}$  of jet pairs (right), before (top) and after (bottom) applying kinematical cuts.

mass of the WW system as discriminating variables, from the expected number of events at 240 GeV we can forecast at least factors of 2 and 10 improvements on the limits of the aQGC parameters  $a_0^W/\Lambda^2$  and  $a_c^W/\Lambda^2$ :  $(-0.47; +0.47) \times 10^{-6} \text{ GeV}^{-2}$  (Fig. 4), in comparison with the latest results derived (without form-factor) in pp collisions at the LHC [9].

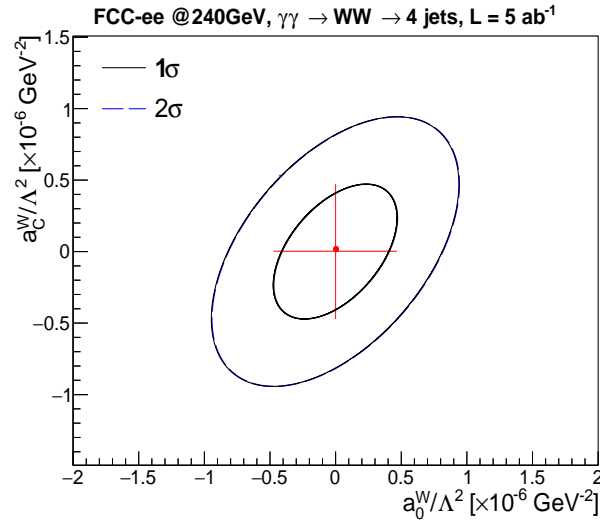


Figure 4: Expected  $1\sigma$  and  $2\sigma$  limits for the anomalous quartic gauge coupling parameters  $a_0^W/\Lambda$  and  $a_c^W/\Lambda$ , from the  $e^+e^- \rightarrow \gamma\gamma \rightarrow W^+W^-(4j)$  measurement at  $\sqrt{s} = 240$  GeV (FCC-ee,  $\mathcal{L}_{\text{int}} = 5 \text{ ab}^{-1}$ ).

## 5 Conclusions

Feasibility studies have been presented for the measurements of the two-photon production of the Higgs boson (in the  $b\bar{b}$  decay channel) as well as of  $W^+W^-$  pairs (in their fully-hadronic decay mode) in  $e^+e^-$  collisions at the FCC-ee, using the equivalent photon flux of the colliding beams. Both final-states are inaccessible at the LHC due to the huge pileup and QCD backgrounds in their full-jet decay channels. Results have been presented for collisions at center-of-mass energies of  $\sqrt{s} = 160, 240, \text{ and } 350$  GeV using SUPERCHIC and PYTHIA 8 Monte Carlo simulations based on the EPA approach, including parton showering, hadronization, and exclusive (2 or 4) jet reconstruction with the  $k_T$  Durham algorithm. Realistic jet reconstruction performances, and (mis)tagging efficiencies are considered, as well as kinematical selection criteria to enhance the signals over the relevant backgrounds. By tagging the outgoing  $e^\pm$  with near-beam detectors ( $\theta_e < 1^\circ$ ), the two-photon  $s$ -channel production of the Higgs boson can be observed with  $5 \text{ ab}^{-1}$  integrated at  $\sqrt{s} = 240$  GeV, where we expect about 75 signal counts on top of 275 counts for the sum of  $\gamma\gamma$  dijet backgrounds. The measurement of  $\gamma\gamma \rightarrow WW \rightarrow 4 \text{ jets}$  will yield several thousands signal events after cuts, that will allow for detailed studies of the trilinear  $\gamma WW$  and quartic  $\gamma\gamma WW$  couplings, improving by at least factors of 2 and 10 the current limits on dimension-6 anomalous quartic gauge couplings. The feasibility analyses developed in this work confirm the novel Higgs and electroweak physics potential open to study through  $\gamma\gamma$  collisions at the FCC-ee.

## Acknowledgments

We thank Lucian Harland-Lang and Ilkka Helenius for useful discussions on SUPERCHIC and PYTHIA 8 respectively. P.R.T acknowledges support from the EDS Blois 2017 organizers and Michelangelo Mangano. This work has granted partially by the Coordination for the Improvement of Higher Education Personnel – CAPES (Brazil).

## References

- [1] S. Chatrchyan *et al.* [CMS Collaboration], Phys. Lett. B **716** (2012) 30.
- [2] G. Aad *et al.* [ATLAS Collaboration], Phys. Lett. B **716** (2012) 1.
- [3] D. d’Enterria, PoS ICHEP **2016** (2017) 434 [arXiv:1701.02663 \[hep-ex\]](#).
- [4] M. Bicer *et al.* [TLEP Design Study Working Group], JHEP **01** (2014) 164; doi:10.1007/JHEP01(2014)164 [arXiv:1308.6176 \[hep-ex\]](#).
- [5] M. L. Mangano *et al.*, CERN Yellow Report (2017) 1; [arXiv:1607.01831 \[hep-ph\]](#).



- [6] D. d’Enterria, Proceeds. 17th Lomonosov Conf. (Moscow, Aug. 2015), World Scientific doi:10.1142/9789813224568\_0028 [arXiv:1602.05043 \[hep-ex\]](#).
- [7] V. M. Budnev et al., Phys. Rept. **15** (1974) 181.
- [8] P. Rebello Teles and D. d’Enterria, Proceeds. PHOTON’15, [arXiv:1510.08141 \[hep-ph\]](#).
- [9] S. Chatrchyan *et al.* [CMS Collaboration], JHEP **07** (2013) 116; doi:10.1007/JHEP07(2013)116 [arXiv:1305.5596 \[hep-ex\]](#); V. Khachatryan *et al.* [CMS Collaboration], JHEP **08** (2016) 119 doi:10.1007/JHEP08(2016)119 [arXiv:1604.04464 \[hep-ex\]](#); M. Aaboud *et al.* [ATLAS Collaboration], Phys. Rev. D **94** (2016) 032011 doi:10.1103/PhysRevD.94.032011 [arXiv:1607.03745 \[hep-ex\]](#).
- [10] A. Dainese *et al.*, CERN Yellow Report (2017) no.3, 635; doi:10.23731/CYRM-2017-003.635 [arXiv:11605.01389 \[hep-ph\]](#).
- [11] M. G. Albrow *et al.* [FP420 R&D Collaboration], JINST **4** (2009) T10001 [arXiv:0806.0302 \[hep-ex\]](#).
- [12] J. Alwall *et al.*, JHEP **07** (2014) 079 [arXiv:1405.0301 \[hep-ph\]](#).
- [13] T. Sjöstrand *et al.*, Comput. Phys. Commun. **191** (2015) 15 [arXiv:1410.3012 \[hep-ph\]](#).
- [14] L. A. Harland-Lang, V. A. Khoze, M. G. Ryskin, Eur. Phys. J. C **76** (2016) 9 [arXiv:11508.02718 \[hep-ph\]](#).
- [15] F. Ferro [CMS and TOTEM Collaborations], AIP Conf. Proc. **1819** (2017) 040019 doi:10.1063/1.4977149.
- [16] T. Sjöstrand, S. Mrenna and P. Z. Skands, JHEP **05** (2006) 026 [arXiv:hep-ph/0603175](#).
- [17] S. Catani, Y. L. Dokshitzer, M. H. Seymour and B. R. Webber, Nucl. Phys. B **406** (1993) 187. doi:10.1016/0550-3213(93)90166-M
- [18] M. Cacciari, G.P. Salam, G. Soyez, E. Phys. J. C **72** (2012) 1896 [arXiv:1111.6097 \[hep-ph\]](#).
- [19] P. Janot private communication; P. Janot and G. Ganis, “The HZHA Generator in Physics at LEP2”, Eds. G. Altarelli, T. Sjöstrand and F. Zwirner, CERN Report 96/01 (Vol.2); <http://cdsweb.cern.ch/record/473529>.
- [20] M. Spira, Nucl. Instrum. Meth. A **389** (1997) 357; A. Djouadi, J. Kalinowski and M. Spira, Comput. Phys. Commun. **108** (1998) 56; A. Djouadi, J. Kalinowski, M. Mühlleitner and M. Spira, [arXiv:1003.1643 \[hep-ph\]](#); <http://people.web.psi.ch/spira/hdecay/>.
- [21] D. d’Enterria, J. P. Lansberg, Phys. Rev. D **81** (2010) 014004 [arXiv:0909.3047 \[hep-ph\]](#).